eISSN: 2721-5717; pISSN: 2747-2124 https://journal.unhas.ac.id/index.php/zonalaut

ZONA LAUT

JOURNAL OF OCEAN SCIENCE AND TECHNOLOGY INNOVATION

# Title: Assessment of Current Energy and Power Generation in the Sunda Strait through Hydrodynamic Modeling with Delft3D and Turbine Evaluation

Suciana[1]*, Elsa Rizkiya Kencana[1], Rayhan Al-Ghazali[1] and Sumartini[2]
Departement of Ocean Engineering. Institut Teknologi Sumatera, Lampung, Indonesia
Departement of Regional dan Urban Planning. Universitas Teknologi Yogyakarta, Yogyakarta, Indonesia
*suciana@kl.itera.ac.id

**Abstract**

Indonesia's rapid population growth has significantly increased energy demand, posing challenges due to the declining availability of fossil fuels, the primary energy source for most power plants. Given its geographical position as a maritime nation, with nearly six million square kilometers of ocean and over 81,000 kilometers of coastline, Indonesia holds immense potential for harnessing ocean currents, waves, and tides for renewable energy development. Exploring these alternative marine energy resources is essential to meeting future energy needs. One of the most promising locations for ocean current power plants is the Sunda Strait. This research aims to model ocean currents in the Sunda Strait using Delft3D software to assess their potential for ocean current power plant development. The study also includes initial mapping of high-potential areas for energy production. Results from three observation points, Sragi, Rimaubalak, and Sangiang, indicate that the waters around Sangiang are the most suitable for ocean current power plants. In 2024, the average current speed was 0.93 m/s, with a maximum reached of 5.20 m/s. For energy generation, the Gorlov turbine proved particularly effective, producing 21,285 kW in 2024 with an efficiency of 36%. The Darrieus turbine produced 18,262 kW in 2024 with an efficiency of 45%. Both turbines are deemed highly viable for further development in the Sunda Strait, offering a significant step toward Indonesia's renewable energy goals.

**Keywords:** Hydrodynamic modeling, Energy, Ocean Current Power Plants, Turbine, Delft3D

## 1. INTRODUCTION

Indonesia has an estimated ocean current energy potential of 75 GW, with around 18 GW considered technically exploitable [1]. However, the country's electricity supply is still predominantly dependent on conventional fossil-based energy. This type of energy is non-renewable and contributes to environmental problems such as pollution and global warming. According to PT PLN (Persero), electricity demand was expected to increase by an average of 8.6% per year between 2016 and 2025. Therefore, more in-depth research is needed to identify alternative energy sources that can replace fossil fuels. One of the most promising sites for ocean current power generation in Indonesia is the Sunda Strait, located in Lampung Province. This strait is one of the busiest maritime passages between Sumatra and Java, playing a vital role in both economic and social activities.

The Sunda Strait, located between the Indian Ocean and the Java Sea, serves as a key passage where seawater masses converge and flow. Previous studies have shown that average current speeds in the strait range from 0.66 to 1.0 m/s, indicating its strong potential for the development of ocean current power plants [2][3][4]. A 2019 study by Nuriyati et al. focused on the area between Peucang Island and Ujung Kulon near the Sunda Strait, analyzing tidal and current data, conducting numerical modeling, and estimating power density. The results showed a maximum current speed of 1.95 m/s, with the highest power density of 4.51 W/m² occurring during ebb-to-flood conditions [5]. In this strait, seawater masses tend to accelerate due to the narrowing passage between the open sea and the strait, which constrains the flow and increases current velocity [6].

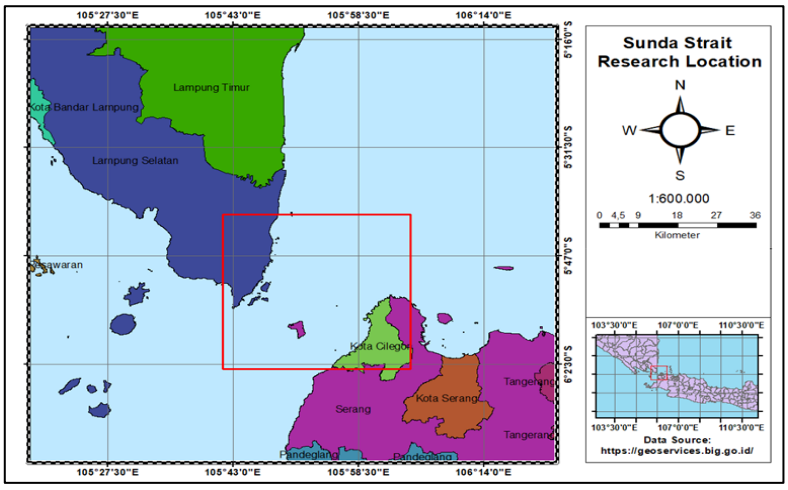

Figure 1. Location of Sunda Strait waters

One effective method to analyze and assess the potential of ocean currents is through hydrodynamic modeling. Hydrodynamic modeling is a scientific approach used to study marine processes and conditions, including waves, currents, and water masses [7][8][9]. This modeling technique allows for the determination of wave height and propagation patterns, the speed and direction of ocean currents, and tidal characteristics [10]. Therefore, the objectives of this research are to model current patterns in the Sunda Strait using Delft3D software, estimate the energy potential of ocean currents, and conduct a preliminary mapping of areas suitable for Ocean Current Power Plant (PLTAL) development in the waters of the Sunda Strait.

## 2. METHODS

### 2.1. Data Collection and Processing Methods

In research, it is important to use appropriate methods to collect the necessary data. Furthermore, data must be managed systematically and scientifically to ensure its reliability and usability. The data used in this study are classified into two types: primary data and secondary data. Secondary data refers to information obtained from official websites and published journals, while primary data is collected directly through field surveys. In this research, tidal and current measurements are used as primary data, while secondary data include coastline data, AVISO-derived current data, and bathymetric information.

### 2.2. Delft-3D Modeling

This study utilized the Delft3D-FLOW module from the open-source Delft3D software. This module is used to simulate and visualize the direction and velocity of ocean currents, which are then analyzed to determine the potential for ocean current power plants in the Sunda Strait. Delft3D is an open-source modeling tool developed by Deltares, designed to study hydrodynamic behavior, sediment transport, waves, morphological and ecological changes, and water quality in coastal environments. Delft3D-FLOW solves the Navier–Stokes equations for incompressible fluids, assuming shallow water conditions and applying the Boussinesq approximation. Vertical acceleration is neglected in the vertical momentum equation, resulting in a hydrostatic pressure approximation. Vertical velocity in the 3D model is derived from the continuity equation. These equations and appropriate initial and boundary conditions are solved on a finite-difference grid. Because the boundaries of rivers, estuaries, and coastal seas are generally curved, they cannot be accurately represented on a standard rectangular grid, potentially leading to discretization errors. To address this, Delft3D-FLOW uses curvilinear orthogonal coordinates that better match the natural boundary shapes. This approach also allows for local grid refinement in areas with strong horizontal gradients [11].

The depth-averaged continuity equation is obtained by integrating the continuity equation for incompressible fluids ($\nabla \cdot u = 0$) over the total depth, taking into account the kinematic boundary conditions at the water surface and the bottom level. The continuity equation can be seen in Equation 2.1

$$\frac{\partial \zeta}{\partial t}+\frac{1}{\sqrt{G^{\xi\xi}.G^{\eta\eta}}}\left(\frac{\partial\left((d+\zeta)U\sqrt{G_{\eta\eta}}\right)}{\partial \xi}+\frac{\partial\left((d+\zeta)V\sqrt{G_{\xi\xi}}\right)}{\partial \eta}\right)=(d+\zeta)Q \quad (2.1)$$

The equations used to determine the momentum for the ξ and η directions are included in Equation 2.2 and 2.3

$$\frac{\partial u}{\partial t}+\frac{u}{\sqrt{G_{\xi\xi}}}\frac{\partial u}{\partial \xi}+\frac{v}{\sqrt{G_{\eta\eta}}}\frac{\partial u}{\partial \eta}+\frac{\omega}{d+\zeta}\frac{\partial u}{\partial \sigma}-\frac{v^2}{\sqrt{G_{\xi\xi}}\sqrt{G_{\eta\eta}}}\frac{\partial \sqrt{G_{\eta\eta}}}{\partial \xi}+\frac{uv}{\sqrt{G_{\xi\xi}}\sqrt{G_{\eta\eta}}}\frac{\partial \sqrt{G_{\xi\xi}}}{\partial \eta}-fv=-\frac{1}{\rho_0\sqrt{G_{\xi\xi}}}P_\xi+F_\xi+\frac{1}{(d+\zeta)^2}\frac{\partial}{\partial \sigma}\left(vv\frac{\partial u}{\partial \sigma}\right)+M_\xi \quad (2.2)$$

$$\frac{\partial v}{\partial t}+\frac{u}{\sqrt{G_{\xi\xi}}}\frac{\partial v}{\partial \xi}+\frac{v}{\sqrt{G_{\eta\eta}}}\frac{\partial v}{\partial \eta}+\frac{\omega}{d+\zeta}\frac{\partial v}{\partial \sigma}+\frac{uv}{\sqrt{G_{\xi\xi}}\sqrt{G_{\eta\eta}}}\frac{\partial \sqrt{G_{\eta\eta}}}{\partial \xi}-\frac{u^2}{\sqrt{G_{\xi\xi}}\sqrt{G_{\eta\eta}}}\frac{\partial \sqrt{G_{\xi\xi}}}{\partial \eta}+fu=-\frac{1}{\rho_0\sqrt{G_{\eta\eta}}}P_\eta+F_\eta+\frac{1}{(d+\zeta)^2}\frac{\partial}{\partial \sigma}\left(vv\frac{\partial v}{\partial \sigma}\right)+M_\eta \quad (2.3)$$

The vertical velocity ω in the σ coordinate is derived from the continuity in Equation 2.4

$$\frac{\partial \zeta}{\partial t}+\frac{1}{\sqrt{G^{\xi\xi}.G^{\eta\eta}}}\left(\frac{\partial\left((d+\zeta)u\sqrt{G_{\eta\eta}}\right)}{\partial \xi}+\frac{\partial\left((d+\zeta)v\sqrt{G_{\xi\xi}}\right)}{\partial \eta}\right)+\frac{\partial \omega}{\partial \sigma}=(d+\zeta)(q-q^{out}) \quad (2.4)$$

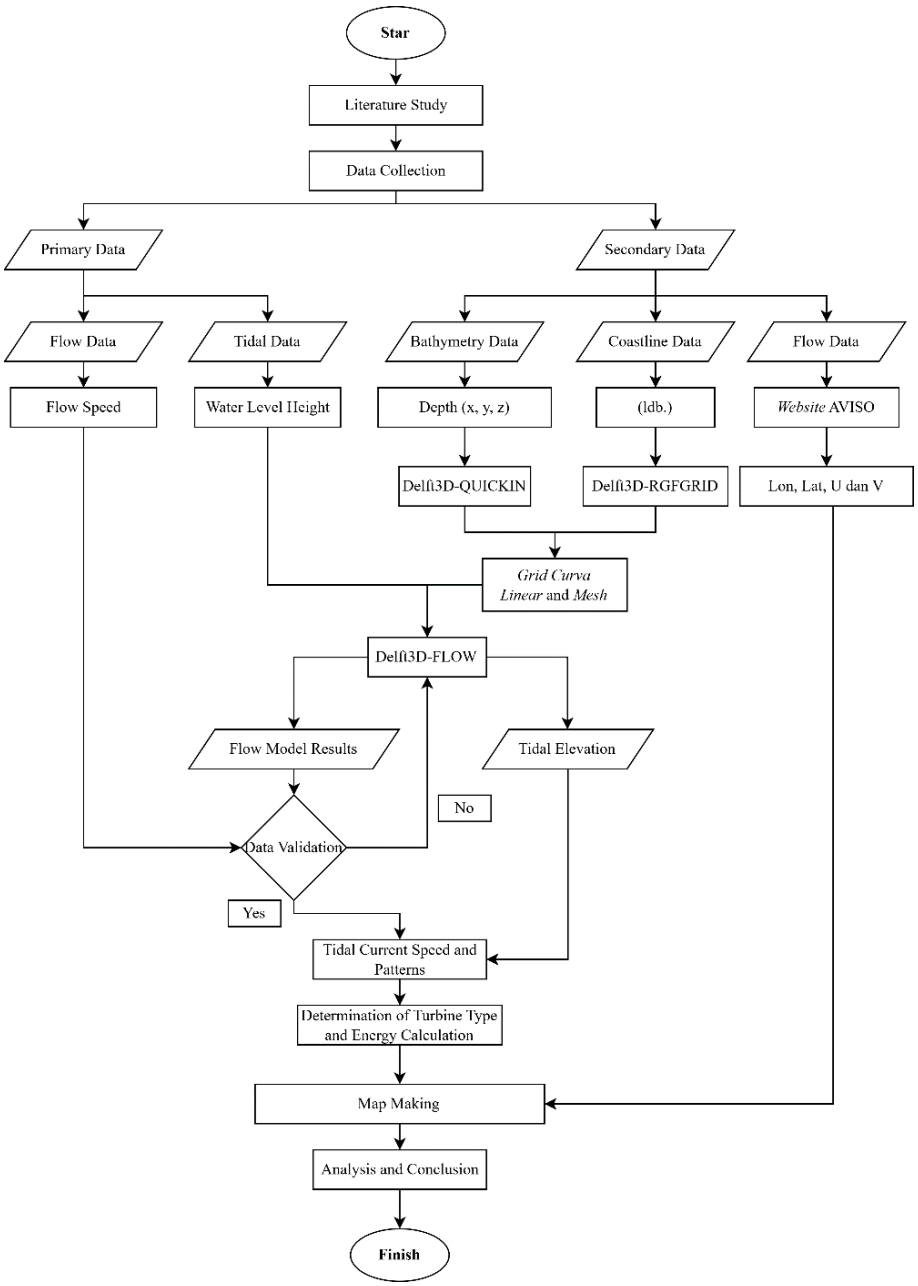


Figure 2. Research Methodology Flow Chart

There are three main steps in hydrodynamic modeling. The first step is data pre-processing, which involves creating meshes at the research location. To create a large net, we have to plan the model by determining observation points (See Figure 3). Then create a grid in the waters of the Sunda Strait (see Figure 4). The grid is defined as a coordinate system that divides the simulation area into small cells used to solve the governing numerical equations. Delft3D Flow utilizes a curvilinear grid, which allows for better representation of complex coastlines and bathymetric features. In this study, the grid resolution ranges from 50 meters in the coastal areas to 300 meters in offshore regions, providing a balance between spatial accuracy and computational efficiency. The grid was constructed based on national bathymetric data.
The second stage is data processing, which includes the Flow module by entering data such as bathymetry, boundaries, and setting the modeling time frame. The open boundary is located on the offshore side and is used to input tidal forcing, derived from TPXO global tidal data. Meanwhile, the closed boundary lies along the land or coastline, where no water exchange occurs, representing a solid, impermeable boundary. The final stage is data processing, which starts from running the model until the model output data is obtained.The simulation was run over a full annual period (1 year) to incorporate seasonal variations in tidal and current behavior, including the influence of monsoonal patterns. The model outputs were generated at 1-hour intervals, which provided sufficient temporal resolution to capture both diurnal tidal cycles and long-term seasonal trends.

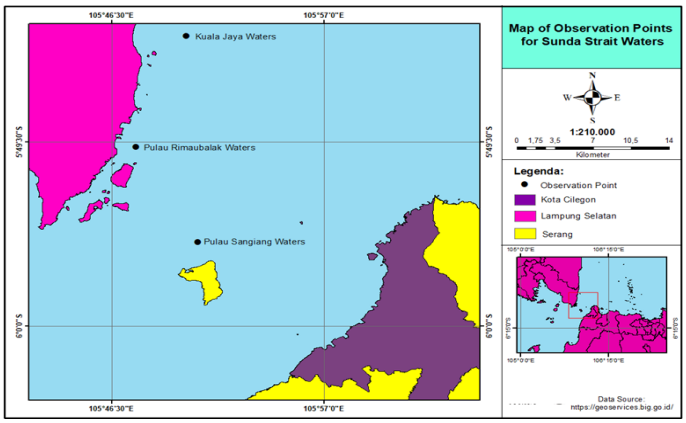

Figure 3. Observation Map

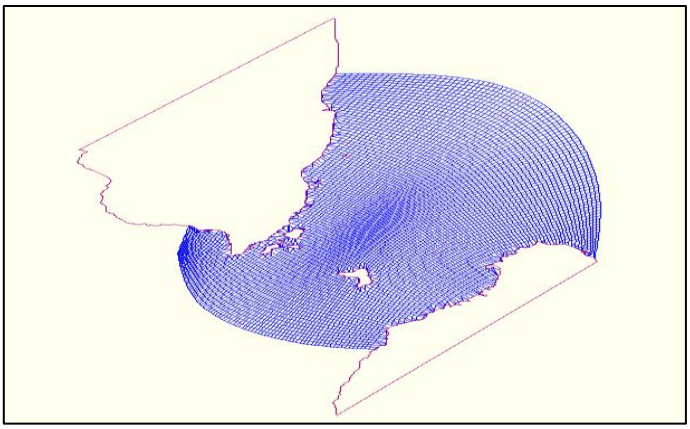
Figure 4. Grid Model

## 2.3. Model Validation Method

The tide model is validated using field recess installation data. The modeling results that have been simulated should be verified using the measurement data directly located at the localization. The purpose of the data verification is to find out the accuracy level of the simulation data with the field data. The method used in data verification is the RMSE (Root Mean Square Error) method. RMSE is used to find the accuracy of predictions with historical data. The advantage of RMSE is that it has a fairly high level of sensitivity. The calculation of RMSE can be seen in Equation 2.5 [12]

$$RMSE = \sqrt{\sum_{i}^{n} \frac{(X_{observasi} - X_{model})^2}{n}} \quad (2.5)$$

Where $X_{obs}$ is field measurement data, $X_{model}$ is result of model data and n is amount of data. according to research [13] using the RMSE formula, the classification of the error rate based on the RMSE value obtained is shown in Table 1.

Table 1. RMSE Value Classification

| RMSE Value | Percentage (%) | Error rate |
|---|---|---|
| 0,00 – 0,299 | 0 – 29 | Small |
| 0,30 – 0,599 | 30 – 59 | Medium |
| 0,60 – 0,899 | 60 – 89 | Large |
| >0.90 | 90 | Very Large |

### 2.4. Tidal Data Processing

The contents of the method can use sub-chapters, if necessary from tidal component data, information regarding tidal types can also be obtained. These tidal types are determined by the value of the Formzahl number in Equation 2.6 [14]

$$F = \frac{(K1 + O1)}{(M2 + S2)} \quad (2.6)$$

There are four tidal types based on what is shown in Table 2

Table 2. Formzahl Number

| Tidal Type | Formzahl Number |
|---|---|
| Semi-Diurnal | $F \leq 0{,}25$ |
| Mixed Semi-Diurnal | $0{,}25 < F \leq 1{,}5$ |
| Mixed Diurnal | $1{,}50 < F \leq 3{,}0$ |
| Diurnal | $F > 3{,}0$ |

Diurnal tides have the characteristic of having one high tide and one low tide in a 24-hour period, while Semi-Diurnal tides have two high tides and two low tides in 24 hours, with a tidal period of 12.4 hours. To calculate the elevation of the water surface due to tidal surges, it is important to use the amplitude values of the tidal component.

### 2.5. Marine current turbine

A marine current turbine is a device used to convert the kinetic energy of ocean currents into electrical energy. Its operating principle is similar to that of a wind turbine, where kinetic energy from seawater movement is converted into electricity. The mechanism is similar to that of a wind turbine: the horizontal movement of seawater rotates the turbine blades connected to a generator, which then converts the motion into electrical energy [15]. Selecting the appropriate type of turbine is essential to match local water conditions and maximize energy output. Based on the hydrodynamic characteristics of the Sunda Strait, two suitable turbine types have been identified: the Darrieus turbine and the Gorlov turbine, as shown in Figure 5.

The Darrieus turbine was developed in 1931 by French aeronautical engineer Georges Jean Marie Darrieus. It offers several advantages, such as low dependence on flow direction due to its symmetrical shape and the ability to operate at low current speeds. However, a major drawback is that it may generate strong vibrations at higher current velocities. With a turbine cross-sectional area of 3 m², the Darrieus turbine can generate 2 kW of electricity at a current speed of 1.4 m/s [16][17].

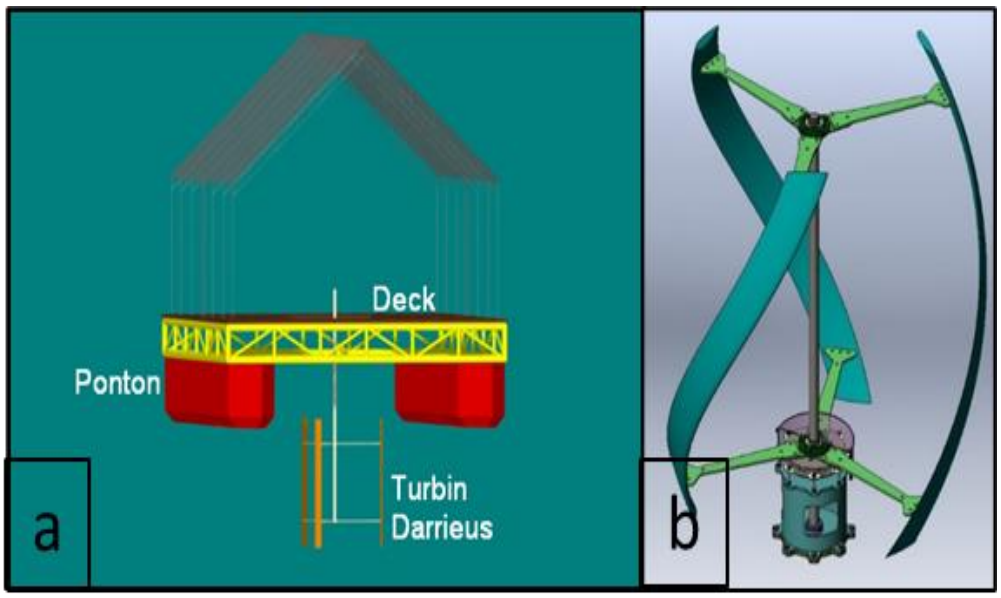

Figure 5. Darrieus turbine (a) and Gorlov Turbine (b)

### 2.6. Energy Calculations

To determine the value of electrical energy from the current speed [18] use the following formula:

$$P = 0.5 \times \eta \times \rho \times A \times V^3 \quad (2.7)$$

The electrical energy produced, denoted as $P$, represents the system's power output and is measured in kilowatts (kW). Turbine efficiency, symbolized by $\eta$, typically ranges between 35% and 45%, indicating the proportion of kinetic energy successfully converted into electrical energy. The specific gravity of water, represented by $\rho$, is 1025 kg/m³. The cross-sectional area of the turbine, denoted as $A$, is measured in square meters (m²) and influences the volume of water interacting with the turbine. Lastly, $V$ refers to the current speed of water flow, expressed in meters per second (m/s), which plays a critical role in determining the available kinetic energy for conversion.

The value of Turbine efficiency use 35% efficiency, was selected as a conservative estimate for small-scale hydrokinetic turbines such as the Darrieus and Gorlov Helical Turbine (GHT). Gorlov [19] demonstrated through experimental testing that the GHT, which is a helical modification of the Darrieus turbine, could reach conversion efficiencies of approximately 35% under free-flow water conditions. This Turbine efficiency is also supported by more recent studies examining the performance of vertical-axis turbines with NACA 0020 airfoil blades under low-speed marine currents [20]. The 45% efficiency was used to represent an optimistic yet realistic scenario, supported by studies on improved Darrieus-type turbines equipped with deflectors and optimized rotor geometry. These improvements allow power coefficients (Cp) to approach or exceed 0.45, corresponding to efficiency levels between 45%–55% depending on flow conditions and design configuration [21][22].

## 3. RESULTS AND DISCUSSION

### 3.1. Tidal

Tidal validation was carried out using the RMSE (Root Mean Square Error) method, the results showed that the error value from tidal validation was 0.10, which was included in the small category. Tide validation starts from July 23 to August 6, 2023. The graphic comparison between field data and model data is shown in Figure 6.

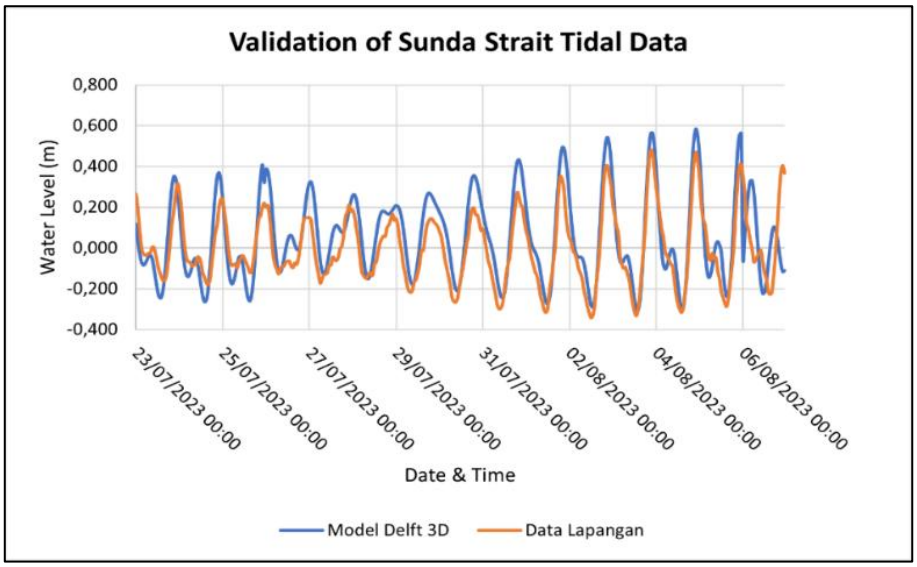

Figure 6. Tidal Model Data

In the research conducted at White Sand Beach, tidal astronomical components were obtained from data processing using the Least Squares method in Table 3.

Table 3. Tidal Astronomical Component

| Tidal Astronomical Component | Sea | |
|---|---|---|
| | Amplitude (cm) | Phase (°) |
| M2 | 21.68 | 109.78 |
| S2 | 10.67 | 79.83 |
| N2 | 4.90 | 105.58 |
| K1 | 8.23 | 275.06 |
| M4 | 0.11 | 119.83 |
| O1 | 4.53 | 46.58 |
| P1 | 2.71 | 275.06 |
| K2 | 2.45 | 79.83 |
| MS4 | 0.03 | 188.45 |

Based on the tidal component values obtained, it is known that the fomzahl number is 0.38, which means a single daily tide or diurnal tide.

### 3.2. Current

The simulated currents are based on tidal conditions, as the hydrodynamic model applies tidal forcing. Tidal modeling is conducted under two conditions: spring tides and neap tides. Spring tides occur when the Earth, moon, and sun are aligned in a straight line, typically during the new moon and full moon phases. This alignment results in the highest high tides and the lowest low tides. Neap tides occur when the Earth, moon, and sun form a 90-degree, typically during the first and third quarter moon phases. This configuration causes the smallest difference between high and low tide levels. The following figure presents the simulated current speed and flow patterns during spring tide conditions, generated using Delft3D software. The flow data from the modeling results in 2024, the average flow value is around 0.938 m/s with a maximum flow of 5.20 m/s and a minimum flow of 0.01 m/s.

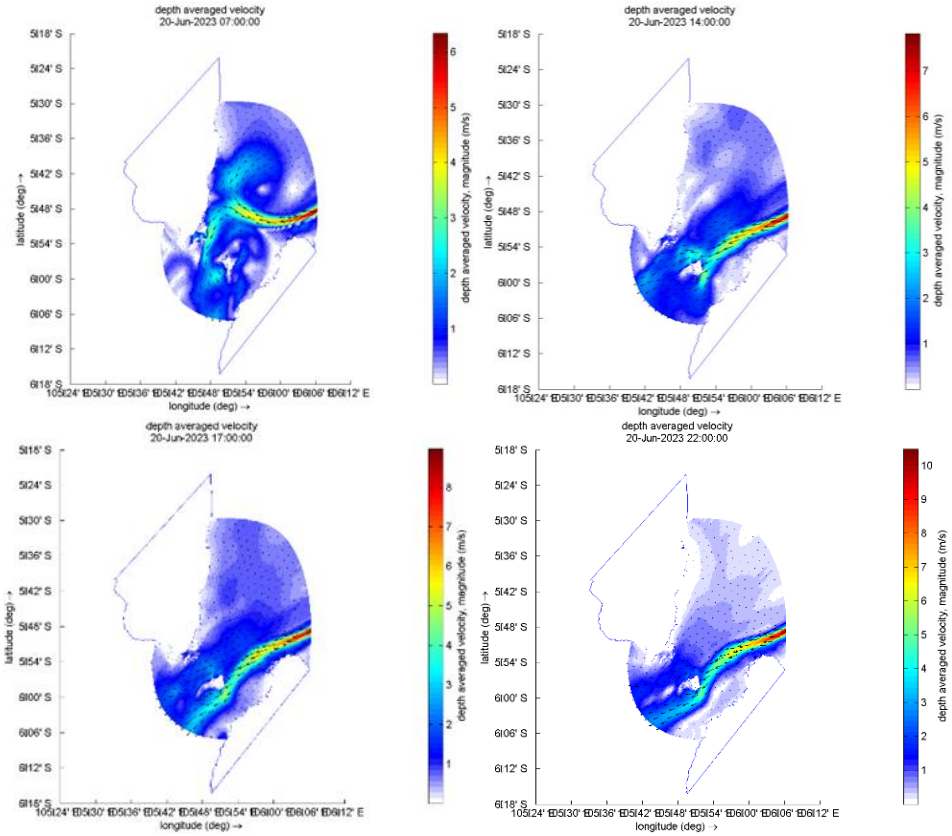


Figure 7. Current Conditions during Full Moon Tide, (A) Ebb towards Tide, (B) Tide, (C) Tide towards Ebb, (D) Ebb

### 3.3. Energy Calculations

Based on theoretical calculations using an efficiency value of 35%, the Darrieus turbine in 2024 is projected to produce a total output power of 100,642 kW. The average output power is 882 kW, with a maximum of 1,367 kW and a minimum of 266 kW. For the Gorlov turbine, the total output power is 21,285 kW, with an average of 1,764 kW, a maximum of 2,735 kW, and a minimum of 533 kW. Two notable peaks in energy production are observed in 2024. The first occurred in June, when the Darrieus turbine reached 1,367 kW and the Gorlov turbine 2,735 kW. The second peak was in December, with the Darrieus turbine producing 1,361 kW and the Gorlov turbine 2,722 kW. These peaks correspond to the highest current velocities recorded during the year, with June reaching a maximum of 5.08 m/s (average 1.06 m/s) and December reaching a maximum of 5.20 m/s with an average current of 1.04 m/s.

Table 4. Turbine Output Power

| Output Power2024 | | |
|---|---|---|
| Month | Turbin Darrieus (KW) | Turbin Gorlov (KW) |
| January | 1167 | 2335 |
| February | 809 | 1618 |
| March | 666 | 1333 |
| April | 669 | 1339 |
| May | 958 | 1917 |
| June | 1367 | 2735 |
| July | 1288 | 2577 |
| August | 995 | 1990 |
| September | 694 | 1388 |
| October | 266 | 533 |
| November | 338 | 677 |
| December | 1361 | 2722 |

| Output Power2024 | | |
|---|---|---|
| Month | Turbin Darrieus (KW) | Turbin Gorlov (KW) |
| Average | 882,06 | 1764,12 |
| Minimum | 266,59 | 533,17 |
| Maximum | 1367,76 | 2735,52 |
| Total | 10642,65 | 21285,31 |

To optimize the output power from each turbine, it is essential to analyze the probability distribution of current speeds. Identify the speed ranges at which each turbine produces maximum power, as well as how frequently these speeds occur in the waters of the Sunda Strait. For the Darrieus turbine, current speeds in the range of 0–0.5 m/s occurred 1,959 times, accounting for 22.46% of the data and producing a total output power of 47.46 kW. Speeds between 0.5–1.0 m/s occurred 3,289 times (37.70%) and generated 790.89 kW, while speeds from 1.0–1.5 m/s occurred 2,468 times (28.29%), yielding 2,510 kW of total output power. It can be concluded that current speeds between 0 and 1.5 m/s are the most dominant in the Sunda Strait, making them critical for turbine performance assessment.

### 3.4. Turbine Type Selection

In selecting a suitable turbine type, detailed calculations are required to evaluate the advantages and disadvantages of each option. These calculations ensure that the chosen turbine meets the expected performance criteria. In this research, the decision table method was used to aid in turbine selection. A decision table is a structured tool that organizes relevant information about each turbine, including performance scores based on predefined criteria. This information is then used as the basis for assigning scores and supporting the selection process. The final scores serve as a reference for determining the most appropriate turbine type, as shown in Table 5.

In the decision table above, turbine selection was based on five criteria: efficiency, output power, design, operational system, and development potential. Each criterion was weighted on a priority scale from 5 to 1, with efficiency as the highest priority, followed by output power, design, operational system, and development as the lowest priority. In terms of efficiency, the Darrieus turbine scored higher (9) compared to the Gorlov turbine (7), due to its superior efficiency of 45.05%, while the Gorlov turbine achieved only 36.52%. Conversely, for output power, the Gorlov turbine outperformed the Darrieus with a score of 10 versus 6, as it reached 18,262 kW compared to Darrieus's 9,131 kW.

Regarding design, the Gorlov turbine scored 7, considered more efficient due to its cylindrical helical shape, while the Darrieus turbine, with a straight-blade design, scored 5. For the operational system, Gorlov again ranked higher with a score of 9, due to its stable performance under various flow conditions. The Darrieus turbine received a score of 8, as it tends to vibrate under high-velocity currents. In terms of development potential, the Darrieus turbine led with a score of 7, as it has already been implemented in tidal energy projects such as in the Larantuka Strait. The Gorlov turbine, still in the research stage, scored 5. By summing the weighted scores, the total score for the Darrieus turbine was 107, while the Gorlov turbine scored 119. Based on this evaluation, the Gorlov turbine was selected as the most suitable option for ocean current power plant (PLTAL) development in the waters of the Sunda Strait.

Table 5. Turbin Type Selection

| Criteria | Priority Factors | Darrieus | PF x Darrieus | Gorlov | PF x Gorlov |
|---|---|---|---|---|---|
| Efficiency | 5 | 9 | 45 | 7 | 35 |
| Output Power | 4 | 6 | 24 | 10 | 40 |
| Desain | 3 | 5 | 15 | 7 | 21 |
| Work system | 2 | 8 | 16 | 9 | 18 |
| Development | 1 | 7 | 7 | 5 | 5 |
| Total Score | | | 107 | | 119 |

### 3.5. Ocean Current Distribution Map

The Sunda Strait has significant potential for the development of Marine Current Power Plants (PLTAL), with current speeds ranging between 1.0 m/s and 2.5 m/s. In the map above, as shown in Figure 8, areas with lower current velocities are represented in dark green, corresponding to a speed range as low as 0.5 m/s. As the green color becomes lighter, it indicates increasing current speeds in those areas.

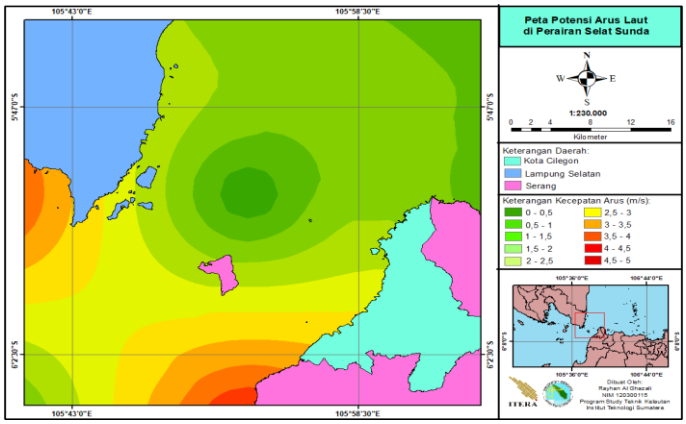

Figure 8. Map of the Distribution of Ocean Currents in the Sunda Strait

### 3.6. Discussion

Uncertainty in this study arises from several interconnected factors. These include limitations in bathymetric data accuracy, potential mismatch between global tidal boundary conditions and local dynamics, and the influence of grid resolution on capturing fine-scale flow features. Numerical assumptions such as constant eddy viscosity and simplified turbulence models can further affect flow simulation, especially near turbine depths. The lack of in situ current validation (e.g., ADCP measurements) introduces additional uncertainty in velocity outputs. Furthermore, power estimations rely on assumed turbine efficiencies (35% and 45%) that may not reflect real-world mechanical and operational losses.

Following well-established hydrodynamic theory, power output from hydrokinetic turbines scales with the cube of the current velocity ($P \propto v^3$), making the system highly sensitive to even small changes in flow speed. For example, a 10% variation in velocity may lead to approximately a 33% variation in power output, as outlined in studies of turbine power density response to flow conditions in riverine and tidal environments [23]. This relationship has been confirmed both analytically and through CFD-based sensitivity evaluations [24]. Therefore, it is critical to ensure accuracy in current modeling and calibration, as minor errors in velocity estimation can result in substantial deviations in projected energy yields. Future work should include a full parametric sensitivity analysis for more robust feasibility assessment.

## 4. Conclusion

The current pattern of the waters of the Sunda Strait mostly moves from the northeast to the southwest, which is characterized by the direction of the current during full and neap tides, which is dominated by the northeast-to-southwest direction. From 3 current observation points, namely in the Sragi, Rimaubalak Island, and Sangiang Island. The waters of Sangiang Island are considered appropriate for developing a Marine Current Power Plant (PLTAL) because they have an average current value of 0.93 and a maximum current of 5.20 in 2024.

The maximum power produced by the Darrieus turbine in 2024 is 18,262 kW with an efficiency of 45%. Then the maximum power produced by the Gorlov turbine in 2024 is 21,285.31 kW with an efficiency of 36%. Carried out using the decision table method with five criteria: efficiency, output power, design, work system, and development. The results were obtained for the Gorlov turbine to have the highest score compared to the Darrieus turbine.

## References

[1] N. A. Pambudi, R. A. Firdaus, R. Rizkiana, D. K. Ulfa, M. S. Salsabila, Suharno, and Sukatiman, "Renewable energy in Indonesia: Current status, potential, and future development", *Sustainability*, vol. 15, no. 3, p. 2342, 2023, doi: 10.3390/su15032342.

[2] L. Mujiasih et al., "Simulation of tidal current speed at the Sunda Strait", *ResearchGate*, Jun. 26, 2024. [Online]. Available: https://www.researchgate.net/figure/Simulation-Tidal-current-speed-at-Sunda-Strait_fig1_381762974 [Accessed: June 14, 2025].

[3] F. Rivantoro and I. S. Arief, "Studi pemilihan desain pembangkit listrik tenaga arus laut (PLTAL) menggunakan metode Analytical Hierarchy Process (AHP)", *Jurnal Teknik ITS*, vol. 4, no. 2, pp. B114–B118, 2016, doi: 10.12962/j23373539.v4i2.15257.

[4] B. Supian, S. Suhendar, and R. Fahrizal, “Studi pemanfaatan arus laut sebagai sumber energi listrik alternatif di wilayah Selat Sunda”, Setrum: Sistem Kendali Tenaga Elektronika Telekomunikasi Komputer, vol. 2, no. 1, pp. 49–57, 2015.
[5] N. Nuriyati, P. Purwanto, H. Setiyono, W. Atmodjo, P. Subardjo, A. Ismanto, and M. Muslim, “Potensi energi arus laut di perairan Selat Sunda”, *Indonesian Journal of Oceanography*, vol. 1, no. 1, pp. 44–51, 2019.
[6] A. Safitri, “Pemanfaatan arus laut untuk penentuan lokasi pembangkit listrik tenaga arus laut di Selat Sunda, Banten”, Bachelor's thesis, Universitas Brawijaya, 2014. [Online]. Available: https://repository.ub.ac.id/133600/ [Accessed: June. 14, 2025].
[7] H. Ajiwibowo and M. B. Pratama, “Hydrodynamic model and tidal current energy potential in Lepar Strait, Indonesia”, *International Journal of Renewable Energy Development*, vol. 11, no. 1, pp. 123–130, 2022, doi: 10.14710/ijred.2022.38545.
[8] F. Novico, F. Setiawan, and Y. A. Tambaru, “Tidal current energy resources assessment in the Patinti Strait, Indonesia”, *International Journal of Renewable Energy Development*, vol. 10, no. 3, pp. 517–525, 2021, doi: 10.14710/ijred.2021.35003.
[9] I. A. H. Aswad, H. D. Armono, S. Rahmawati, A. Ridlwan, and R. M. Ariefianto, “Pemodelan tinggi gelombang untuk kajian energi gelombang laut di perairan barat Provinsi Lampung”*, Wave: Jurnal Ilmiah Teknologi Maritim*, vol. 15, no. 2, pp. 75–84, Dec. 2021, doi: 10.29122/jurnalwave.v15i2.4958.
[10] A. Kurniawan, M. Azmiwinata, M. B. Pratama, and C. Kusuma, “Tidal current power in Capalulu Strait, North Maluku: A feasibility study”, *International Journal of Renewable Energy Development*, vol. 13, no. 3, pp. 375–385, May 2024, doi: 10.61435/ijred.2024.60132.
[11] Deltares, “User Manual Delft3D-FLOW: Simulation of Multi-Dimensional Hydrodynamic Flows and Transport Phenomena, Including Sediments”, Delft, The Netherlands: Deltares, 2016.
[12] D. Astari, S. Ibrahim, and R. H. Sihotang, “Analisis pasang surut perairan Dumai menggunakan metode Admiralty”, *Jurnal Online Mahasiswa Fakultas Teknik*, vol. 5, no. 2, pp. 1–7, 2018.
13] F. H. Putra and D. G. Pratomo, “Analisis arus dan transpor sedimen menggunakan pemodelan hidrodinamika 3 dimensi (studi kasus: Teluk Ambon, Kota Ambon, Maluku”, *Jurnal Teknik ITS*, vol. 8, no. 2, pp. A124–A129, 2019, doi: 10.12962/j23373539.v8i2.51760.
[14] C. R. Handoko, M. Mukhtasor, and E. S. Koenhardono, “Performance evaluation of permanent magnet synchronous generator (PMSG) on tidal power generation optimization”, *IOP Conference Series: Earth and Environmental Science*, vol. 1166, no. 1, art. 012023, 2023, doi: 10.1088/1755-1315/1166/1/012023.
[15] W. A. Prayoga and R. Permatasari, “Perancangan dan pemodelan turbin Darrieus untuk pembangkit listrik tenaga arus laut (PLTAL)”, *MESIN: Jurnal Ilmiah Teknik Mesin*, vol. 10, no. 1, pp. 1–8, 2019, doi: 10.24114/mesin.v10i1.12750.
[16] D. D. A. Irfanto, “Studi perancangan combined marine power plant berbasis kombinasi Gorlov helical turbine dengan linear generator di Selat Sunda”, Doctoral dissertation, Institut Teknologi Sepuluh Nopember, 2020.
[17] A. A. Arafat and Y. Arafat, “Assessment of tidal energy resources in Bali Strait, Riset Sains dan Teknologi Kelautan”, vol. 6, no. 2, pp. 125–133, Nov. 2023, doi: 10.62012/sensistek.v6i2.31737.
[18] A. Y. C. Nee, “Power from marine currents, in Proceedings of the 3rd International Conference on Power Electronics Systems and Applications”, Hong Kong, 2009.
[19] A. M. Gorlov, “Limits of the Turbine Efficiency for Free Flow Systems”, *Journal of Energy Resources Technology*, vol. 123, no. 4, pp. 311–317, Dec. 2001.
[20] M. A. Elbatran, M. Y. M. Ali, and A. A. Ahmad, “Assessment of Gorlov helical turbine performance with NACA 0020 blades in low flow water currents”, *International Journal of Hydrogen Energy*, vol. 47, no. 62, pp. 26180–26191, 2022.
[21] S. Karthikeyan, B. S. Pradeep, and D. Selvakumar, “Performance enhancement of Darrieus vertical axis wind turbine using deflector plates”, *Renewable Energy*, vol. 198, pp. 733–744, 2022.
[22] A. Rezaeiha, I. Montazeri-Gh, and D. Danao, “Performance and wake of a vertical axis wind turbine: CFD analysis with different turbulence models”*, Renewable Energy*, vol. 107, pp. 1–17, 2017.
[23] [25] J.U. Wiesemann, B. Lehmann, and W. Awandu, “Application of low-cost hydrokinetic technology for accelerating electricity access to rural areas in developing economies: Field experiment in Kenya”, *International Journal of Green Energy*, Nov. 2024, doi: 10.1080/15435075.2024.
[24] S. Chawdhary et al., “Multi-resolution large-eddy simulation of an array of hydrokinetic turbines in a field-scale river,” *The Roosevelt Island Tidal Energy project in New York City* , 2018.